Coherent backscattering reveals the Anderson transition

S. Ghosh,[1, 2] D. Delande,[1] C. Miniatura,[3, 2, 4, 5] and N. Cherroret[1, *]

[1]*Laboratoire Kastler Brossel, UPMC-Sorbonne Universités, CNRS,*
ENS-PSL Research University, Collège de France, 4 Place Jussieu, 75005 Paris, France
[2]*Centre for Quantum Technologies, National University of Singapore, 3 Science Drive 2, Singapore 117543, Singapore*
[3]*MajuLab, CNRS-UNS-NUS-NTU International Joint Research Unit, UMI 3654, Singapore*
[4]*Department of Physics, National University of Singapore, 2 Science Drive 3, Singapore 117542, Singapore*
[5]*INLN, Université de Nice-Sophia Antipolis, CNRS; 1361 route des Lucioles, 06560 Valbonne, France*

We develop an accurate finite-time scaling analysis of the angular width of the coherent backscattering (CBS) peak for waves propagating in 3D random media. Applying this method to ultracold atoms in optical speckle potentials, we show how to determine both the mobility edge and the critical exponent of the Anderson transition from the temporal behavior of the CBS width. Our method could be used in experiments to fully characterize the 3D Anderson transition.

PACS numbers: 05.60.Gg, 42.25.Dd, 72.15.Rn, 03.75.-b

In disordered media, the absence of diffusion arising from the spatial localization of single-particle states is known as Anderson localization (AL) [1]. In three dimensions, AL manifests itself as a phase transition, which occurs at a critical energy, the mobility edge (ME), separating a metallic phase where states are spatially extended, from an insulating one where states are localized. Theoretically, much efforts have been devoted to the study of the critical properties of the Anderson transition, such as wave functions at the ME [2, 3] or critical exponents [4]. In practice however, only a handful of experiments have found evidence for the three-dimensional (3D) Anderson transition [5–10]. For matter waves, its critical (universal) features have been only investigated in the context of quantum-chaotic dynamical localization [11], but no such experiment in 3D disordered potentials has been reported to date.

In addition to the intrinsic difficulty of achieving wave localization in three dimensions, one reason for the rareness of experimental characterizations of the Anderson transition lies in the lack of easily measurable observables displaying criticality. In the context of atom optics, a routinely used approach consists in tracing the evolution in time of the spatial width of a spreading wave packet [7–10]. While AL implies a saturation of the width, the contrary is not true as classical effects can as well entail a saturation or a slowing down in time [12]. Furthermore, atomic wave packets have rather large energy distributions even when cooled down to very low temperatures, which forbids an accurate resolution of the critical region around the ME. Thus, any exploration of the Anderson transition with cold atoms should ideally be complemented with a clear demonstration of phase coherence, and should achieve a good energy resolution. For the latter issue, a first step has been reached in recent measurements of the ME based on a frequency modulation of the disorder [9] – although the experimentally

measured ME seems significantly higher than the one predicted from extensive numerical calculations [13, 14] – and upcoming experiments are moving toward a genuine filtering of the energy distribution, required to access the critical properties of the transition [15]. For additionally proving genuine phase-coherent scattering, the coherent backscattering (CBS) effect is a promising tool. CBS has already been observed in several experiments with cold atoms [16], light [17, 18], acoustic [19] or seismic waves [20] in the (metallic) regime of diffusive transport. Interestingly however, CBS shows up not only in the metallic phase, but all the way across the Anderson transition. The question then naturally arises whether the CBS peak itself could be used as an observable for accessing the critical properties of this transition, in which case one would simultaneously ensure phase coherence.
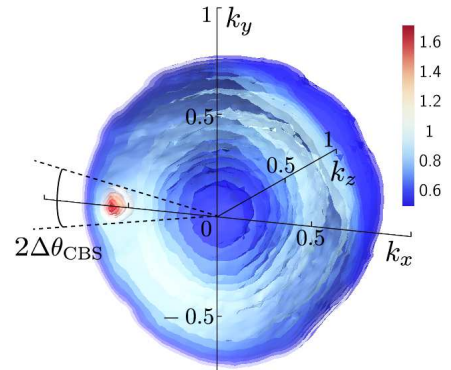

FIG. 1. (color online) Contour plot of the averaged momentum distribution of a matter wave, obtained after propagation of a plane wave $|\boldsymbol{k}_0\rangle$ ($\boldsymbol{k}_0 = 0.6\hat{\boldsymbol{e}}_x$) in a speckle potential of strength $V_0 = 1$ for a duration $t = 800$. The propagated state is here filtered around energy $E = -0.4$ (metallic regime). The CBS peak, of angular width $2\Delta\theta_{\mathrm{CBS}}$, is visible at $\boldsymbol{k} = -\boldsymbol{k}_0$. Here momenta, energies and times are respectively in units of ζ^{-1}, $\hbar^2/(m\zeta^2)$ and $m\zeta^2/\hbar$, where ζ is the correlation length of the potential.

* Corresponding author: cherroret@lkb.upmc.fr

In continuous-wave optical experiments, it is known

that the CBS lineshape changes at the critical point [21]. Unfortunately, this feature is usually smoothed by absorption or finite-size effects and cannot be used in practice. In this letter, we explore the dynamics of the CBS effect *in momentum space* – in contrast with usual setups that search in configuration space – around the Anderson transition. By scrutinizing the dynamics of the CBS angular width, $\Delta\theta_{\mathrm{CBS}}$, in combination with a numerical filter that provides a high energy resolution, we demonstrate that $\Delta\theta_{\mathrm{CBS}}$ can be used to characterize the critical properties of the Anderson transition. By developing an accurate finite-time scaling analysis of the CBS data, we verify the one-parameter scaling theory of localization [22], locate precisely the ME and extract the critical exponent of the transition. We determine these parameters for a speckle potential, and find a good agreement with the predictions of the transfer-matrix method.

As shown in [23], CBS of cold atoms can be observed by tracing the evolution a quasi-plane matter wave in momentum space, a proposal recently realized experimentally [16]. Let us thus consider a matter wave initially prepared in the plane-wave state $|\psi(t=0)\rangle = |\boldsymbol{k}_0\rangle$, and subjected to a 3D random potential $V(\boldsymbol{r})$. Following experiments, we choose $V(\boldsymbol{r})$ to have the statistical properties of a blue-detuned speckle pattern. It is customary to shift all energies by the average value $V_0 > 0$ of the speckle potential, leading to the on-site distribution $P(V) = \exp[-(V + V_0)/V_0]\Theta(V + V_0)/V_0$ (Θ is the Heaviside function), and the two-point correlation function $\overline{V(\boldsymbol{r})V(\boldsymbol{r}')} = V_0^2[\sin(|\boldsymbol{r} - \boldsymbol{r}'|/\zeta)/(|\boldsymbol{r} - \boldsymbol{r}'|/\zeta)]^2$, where ζ is the correlation length. In order to accurately pinpoint the ME E_c, it is useful to restrict the evolution to a narrow energy range ($\pm\sigma$) centered at a given value E that we wish to tune around the E_c, by applying a Gaussian filter [24] $\exp[-(\hat{H} - E)^2/(2\sigma^2)]$ (where $\hat{H} = \hat{\mathbf{p}}^2/(2m) + V(\mathbf{r})$) on the initial state $|\boldsymbol{k}_0\rangle$. This filter makes it possible to accurately extract E_c which otherwise would be smoothed by the natural energy distribution of the initial plane wave in presence of the disordered potential [9, 25]. Throughout this Letter, lengths, momenta, energies and times are given in units of ζ, ζ^{-1}, $\hbar^2/(m\zeta^2)$ and $m\zeta^2/\hbar$, respectively. We discretize the Hamiltonian $\hat{H}$ on a 3D grid of total volume $(60 \times \pi\zeta)^3$ with periodic boundary conditions. Each cell of size $\pi\zeta$ is divided into 2 steps in all three directions. In the following, we use $V_0 = 1, \sigma = 0.02, k_0 = 0.6$.

The temporal evolution and the filtering are performed using a Chebyshev scheme. The evolution operator over Δt, $e^{-i\hat{H}\Delta t/\hbar}$ [resp. the filtering operator] can be expanded in a series of Chebyshev polynomials of the first kind of $a\hat{H}+b$ [resp. $a(\hat{H}-E)^2+b$] with a, b conveniently chosen parameters – see [26, 27] for details – whose coefficients are Bessel [resp. modified Bessel] functions of argument proportional to Δt. The temporal evolution can be computed by iterating small time steps, each involving a limited number of terms in the Chebyshev expansion. The momentum wavefunction is obtained by Fourier transforming the final wave function $|\psi(t)\rangle$.

The procedure is repeated over 6×10^3 configurations of $V(\boldsymbol{r})$, yielding the averaged momentum distribution $\overline{n}(\boldsymbol{k}, t) = \overline{|\langle\boldsymbol{k}|\psi(t)\rangle|^2}$. We show in Fig. 1 the numerical distribution $\overline{n}(\boldsymbol{k}, t)$ obtained at long times for an energy $E = -0.4$ which lies in the metallic regime $E > E_c$. $\overline{n}(\boldsymbol{k}, t)$ clearly displays a narrow interference peak of angular width $\Delta\theta_{\mathrm{CBS}}$ and centered at $\boldsymbol{k} = -\boldsymbol{k}_0$ (in red in Fig. 1). This CBS peak sits on the top of a time-independent isotropic background (in blue in Fig. 1), which in three dimensions has the shape of a spherical shell as a result of elastic multiple scattering off the random potential [23].
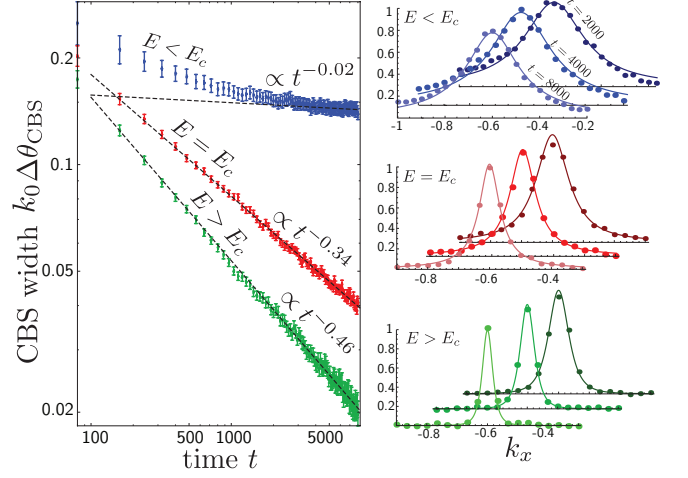

FIG. 2. (color online) Dynamics of the CBS peak across the Anderson transition. Left panel: angular width $\Delta\theta_{\mathrm{CBS}}$ versus time, in the metallic regime $E = -0.4 > E_c$ (green points), at the mobility edge $E = E_c \simeq -0.48$ (red points), and in the insulating regime $E = -0.56 < E_c$ (blue points). Right panels: cut along k_x of the normalized CBS profile at three different energies. For each energy, profiles at three different times $t = 2000, 4000$ and 8000 are displayed, shifted with respect to each other for clarity. The CBS width rapidly saturates in the insulating regime, while it shrinks in time in the metallic and critical regimes. We find an excellent agreement with the temporal dependences predicted by Eq. (1).

We now study the time dependence of the CBS angular width, $\Delta\theta_{\mathrm{CBS}}$. Qualitatively, CBS is an interference effect between two waves that propagate along an identical multiple scattering sequence $\boldsymbol{r}_1 \ldots \boldsymbol{r}_N$ but in opposite directions [28]. The interference term between these paths is proportional to $\overline{\cos[(\boldsymbol{k}_0 + \boldsymbol{k}) \cdot (\boldsymbol{r}_N - \boldsymbol{r}_1)]}$. Therefore, denoting by $\Delta\theta$ the angle (assumed small) between $\boldsymbol{k}$ and $-\boldsymbol{k}_0$, we infer that an interference is visible on average provided $k_0\Delta\theta\Delta r(t) \ll 1$, where $\Delta r(t) = (\overline{|\boldsymbol{r}_N(t) - \boldsymbol{r}_1|^2})^{1/2}$. We thus estimate the angular width of the CBS at a given time t to be $\Delta\theta_{\mathrm{CBS}} \sim 1/[k_0\Delta r(t)]$. The average distance between the first and last points of the scattering sequence depends on the nature of transport in the system. In the metallic regime $E > E_c$, $\Delta r(t) \propto \sqrt{D(E)t}$ with $D(E)$ the diffusion coefficient

at energy E, while $\Delta r(t) \propto t^{1/3}$ at $E = E_c$ [29] and $\Delta r(t) \propto \xi(E)$, the localization length, in the insulating regime $E < E_c$. We thus have:

$$k_0 \Delta\theta_{\mathrm{CBS}} \sim \begin{cases} 1/\sqrt{D(E)t} & E > E_c \\ 1/t^{1/3} & E = E_c \\ 1/\xi(E) & E < E_c. \end{cases} \quad (1)$$

The time dependence of $\Delta\theta_{\mathrm{CBS}}$ is thus qualitatively different in the three regimes of transport. In particular, a sub-diffusive behavior of the CBS width marks the position of the ME E_c. We have performed numerical simulations of the momentum distribution for various energies E around $E_c \simeq -0.48$. We show in the left panel of Fig. 2 the CBS width as a function of time, for three different energies around E_c. At long times, the results follow very well the predictions of Eq. (1). For each energy, we have obtained $\Delta\theta_{\mathrm{CBS}}$ by first removing the isotropic background [24] from the 3D momentum distribution, then fitting the resulting momentum profile with $\alpha/[1 + (\boldsymbol{k} + \boldsymbol{k}_0)^2/\beta]^\gamma$ (where α, β and γ are time- and energy-dependent fit parameters), and finally taking the half width at half maximum of the fitting function. Error bars on $\Delta\theta_{\mathrm{CBS}}$ have been estimated from the standard deviations of β and γ. We show examples of CBS profiles and the corresponding fits in the right panel of Fig. 2.
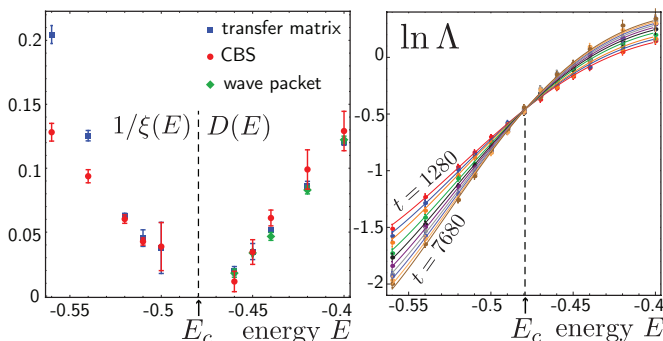

FIG. 3. (color online) Left panel: diffusion coefficient (in the metallic regime $E > E_c$), and inverse of the localization length $1/\xi(E)$ (in the insulating regime $E < E_c$) versus energy E. Red dots are obtained from an analysis of the CBS width, blue squares from the transfer-matrix method, and green diamonds from the spatial spreading of a wave packet. Right panel: scaling function Λ versus energy around the ME, for various times ranging from $t = 1280$ to $t = 7680$. The curves cross at a common point $E_c \approx -0.48$, which signals the location of the ME. Points are the results of numerical simulations of CBS, while solid curves are fits of these data using Eq. (3).

According to Eq. (1), the CBS width is also proportional to the square root of the diffusion coefficient $D(E)$ in the metallic regime, and to the inverse of the localization length $1/\xi(E)$ in the insulating regime, which suggests an original way of measuring these quantities experimentally. To demonstrate the efficiency of such an approach, we have extracted $D(E)$ and $1/\xi(E)$ from the

numerical data for $\Delta\theta_{\mathrm{CBS}}$, by extrapolating the quantities $1/[(k_0\Delta\theta_{\mathrm{CBS}})^2 t]$ (for $E > E_c$) and $1/(k_0\Delta\theta_{\mathrm{CBS}})$ (for $E < E_c$) to infinite times. The results are shown as red dots in the left panel of Fig. 3, for various energies around E_c (no values too close to E_c are shown due to the lack of accuracy of the extrapolation procedure at these energies. The vicinity of E_c deserves a special analysis that will be described below). We have computed these quantities using the transfer-matrix method (blue squares) [30]. In the metallic region, we have also computed $D(E)$ by yet another method that consists in analyzing the spatial width of a spreading, initially narrow wave packet as a function of time (green diamonds). All the results for $D(E)$ are in very good agreement. The predictions below E_c tend to deviate far from the ME, which we explain by the difference in the definition of $\xi(E)$ in the two methods: the localization length that appears in $\Delta\theta_{\mathrm{CBS}}$ controls the exponential decay of the average density, whereas the localization length that appears in transfer matrices controls the exponential decay of the average of the logarithm of the transmission [30].

Let us now explore the behavior of $\Delta\theta_{\mathrm{CBS}}$ in the close vicinity of E_c. In this region, $D(E) \propto |E - E_c|^s$ and $\xi(E) \propto |E - E_c|^{-\nu}$, where the two critical exponents ν and s turn out to be equal for the Anderson transition in dimension 3 [31]. Near E_c, the three scaling laws (1) can be recast under the unified form

$$\Lambda \equiv \frac{1}{Lk_0\Delta\theta_{\mathrm{CBS}}} = F\left[\chi_r(E)L^{1/\nu}\right], \quad (2)$$

where $\chi_r(E) \propto E - E_c$, $L = [t/(2\pi\hbar\rho(E))]^{1/3}$ with $\rho(E)$ the density of states per unit volume at energy E, and F is a function characteristic of the transition. Although the system a priori depends on two parameters E and t, Eq. (2) thus suggests that Λ is in fact a function of a *single* parameter, and is therefore a good candidate for developing a single-parameter scaling description of the Anderson transition [22]. The introduction of the length scale L [32] allows us to establish a straightforward analogy with the usual scaling theory of Anderson localization for time-independent disordered systems [4, 22]. A direct consequence of Eq. (2) is that when $\ln\Lambda$ is plotted against E, the curves at different times should cross at $E = E_c$. This behavior is well visible in the right panel of Fig. 3. By pinpointing the location of the crossing, we obtain a first estimation of the ME: $E_c \simeq -0.48$.

Guided by the one-parameter scaling theory of Anderson localization [22], we now postulate that Eq. (2) holds not only in the close vicinity of the ME [where $\chi_r(E) \propto E - E_c$] but also away from it, and propose to verify this hypothesis by a rigorous finite-size scaling analysis of the numerical data for the CBS width. For this purpose, we introduce a fitting function of the data by Taylor expanding Eq. (2) up to a certain order n_R [4],

$$\Lambda = \sum_{n=0}^{n_R} \chi_r(E)^n L^{n/\nu} F_n, \quad (3)$$

and further expand the variable $\chi_r(E)$ according to

$\chi_r(E) = \sum_{m=1}^{m_R} b_m (E_c - E)^m$. In this model, F_n, b_m, ν and E_c are free parameters. We determine them using a least-square fit of the data for Λ with Eq. (3) retaining data only for sufficiently long times (such that $L > 20$). We show in the right panel of Fig. 3 the results of this fit for curves $\ln \Lambda$ versus E (solid lines). We used $n_R = 2$, $m_R = 3$ (that is 7 fitting parameters) for 1141 data points. The χ^2 per degree of freedom is found to be 0.55. This small value (from the statistical significance point of view) comes from the fact that the data got at the same energy, but different sizes (i.e. different times), are obtained using the same realizations of the disordered potential and thus have residual correlations. We have also tried to include irrelevant scaling variables to better account for deviations to scaling expected at short times [4, 33], but we did not observe significant improvements of the quality of the fits.
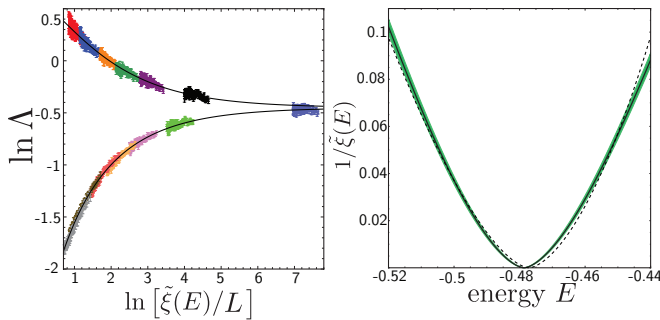

FIG. 4. (color online) Left panel: scaling function Λ constructed by fitting the data for Λ with model (3). Points are the data, and the solid black curve is the fit. All data lie on the same master curve, in agreement with the one-parameter scaling hypothesis, Eq. (2). Right panel: $1/\tilde{\xi}(E) = |\chi_r(E)|^{\nu}$ versus energy E (solid curve), together with the confidence interval (shadowed region, green online). $1/\tilde{\xi}(E)$ vanishes at the ME, and is proportional to $|E - E_c|^{\nu}$ in its vicinity. The dashed curve is the prediction obtained from an independent finite-size scaling analysis based on the transfer-matrix approach.

We then plot the data $\ln \Lambda$ as a function of $\tilde{\xi}(E)/L$, where $\tilde{\xi}(E) = |\chi_r(E)|^{-\nu}$ (colored points), together with the fit to model (3) (solid curve). The results are shown in the left panel of Fig. 4. We see that all data collapse almost perfectly on the same master curve. This result demonstrates that the function Λ, as computed from the width of the CBS peak, does follow the one-parameter scaling theory, in full agreement with Eq. (2). The quantity $\tilde{\xi}(E)$ is proportional to the localization length $\xi(E)$ on the insulating side of the transition, and proportional to the inverse of the diffusion coefficient, $1/D(E)$, on the metallic side. In the right panel of Fig. 4 we show $1/\tilde{\xi}(E)$ as a function of energy, as obtained from the fitting procedure. As expected, $1/\tilde{\xi}(E)$ vanishes at $E = E_c$, which signals the divergence of the localization length and the vanishing of the diffusion coefficient. The fitting analysis also allows us to provide estimations of E_c and of the critical exponent ν. We find $E_c = -0.4786 \pm 13.10^{-4}$ and $\nu = 1.61 \pm 0.03$. Because the above-mentioned chi-squares are too small, they cannot be used to extract the uncertainty. We have thus divided the whole configuration sample in several independent subsets, and estimated E_c and ν for each subset. The reported uncertainties reflect the deviations between the different subsets. They are found to weakly depend on σ, most probably because the finite size scaling approach relies on data belonging to an energy interval much larger than σ. In the right panel of Fig. 4, we also display as a dashed curve the quantity $\tilde{\xi}(E)$ computed from an independent finite-size scaling analysis based on the transfer-matrix method [4, 33]. The latter provides $E_c = -0.4771 \pm 7.10^{-4}$ and $\nu = 1.62 \pm 0.03$, in a somewhat surprisingly good agreement with the estimations extracted from the CBS width. The slight discrepancy from the recently reported value $E_c = -0.43$ [13] comes from the crude discretization we used to save computer resources. Indeed, as involving a time propagation and a narrow energy filter, the characterization of the Anderson transition from the CBS peak is more numerically demanding than from the transfer-matrix approach. Due to this discretization the free-space dispersion relation deviates from the massive one $E = k^2/2$ and $\rho(E)$ is overestimated near the ME, lowering E_c. This shift has however no effect on the physics of the CBS effect or on the Anderson transition.

In conclusion, we have shown that the dynamics of the CBS peak can be used to characterize the Anderson transition, enabling to (i) accurately pinpoint the location of the ME (ii) access the critical exponent and (iii) test the validity of the single-parameter scaling hypothesis. Our method has the double advantage to be based on a physical observable –the CBS peak– which is usually well controlled in experiments, and to demonstrate phase coherence, which is a crucial requirement prior any claim for Anderson localization. The approach has straightforward applications to the field of atom optics in disordered potentials, but it can also be applied to the context of localization of classical waves [5].

[1] P. W. Anderson, Phys. Rev. **109**, 1492 (1958).

[2] A. Rodriguez, L. J. Vasquez, and R. A. Römer, Phys. Rev. Lett. **102**, 106406-4 (2009).

[3] I. S. Burmistrov, S. Bera, F. Evers, I. V. Gornyi, and A.D. Mirlin, Annals of Phys. **326**, 1457 (2011).

[4] K. Slevin and T. Ohtsuki, New J. Phys. **16**, 015012 (2014).

[5] H. Hu, A. Strybulevych, J. H. Page, S. E. Skipetrov, and B. A. van Tiggelen. Nature Phys. **4**, 945 (2008).

[6] A. Aubry, L. A. Cobus, S. E. Skipetrov, B. A. van Tiggelen, A. Derode, and J. H. Page, Phys. Rev. Lett. **112**, 043903, (2014).

[7] F. Jendrzejewski, A. Bernard, K. Müller, P. Cheinet, V. Josse, M. Piraud, L. Pezzé, L. Sanchez-Palencia, A. Aspect, and P. Bouyet, Nature Phys. **8**, 398 (2012).

[8] S. S. Kondov, W. R. McGehee, J. J. Zirbel, and B. De-Marco, Science **334**, 66 (2011).

[9] G. Semeghini, M. Landini, P. Castilho, S. Roy, G. Spagnolli, A. Trenkwalder, M. Fattori, M. Inguscio, and G. Modugno, Nature Phys. **11**, 554 (2015).

[10] J. Chabé, G. Lemarié, B. Grémaud, D. Delande, P. Szriftgiser, and J. C. Garreau, Phys. Rev. Lett. **101**, 255702 (2008).

[11] G. Lemarié, H. Lignier, D. Delande, P. Szriftgiser, and J. C. Garreau, Phys. Rev. Lett. **105**, 090601 (2010).

[12] C. A. Müller and B. Shapiro, Phys. Rev. Lett. **113**, 099601 (2014).

[13] D. Delande and G. Orso, Phys. Rev. Lett. **113**, 060601 (2014).

[14] E. Fratini and S. Pilati, Phys. Rev. A **91**, 061601 (2015).

[15] V. Josse, private communication.

[16] F. Jendrzejewski, K. Müller, J. Richard, A. Date, T. Plisson, P. Bouyer, A. Aspect, and V. Josse, Phys. Rev. Lett. **109**, 195302 (2012).

[17] M. P. Van Albada and A. Lagendijk, Phys. Rev. Lett. **55**, 2692 (1985); P.-E. Wolf and G. Maret, ibid. **55**, 2696 (1985).

[18] G. Labeyrie, F. de Tomasi, J.-C. Bernard, C. A. Müller, C. Miniatura, and R. Kaiser, Phys. Rev. Lett. **83**, 5266 (1999).

[19] G. Bayer and T. Niederdränk, Phys. Rev. Lett. **70**, 3884 (1993); A. Tourin, A. Derode, P. Roux, B. A. van Tiggelen, and M. Fink, ibid. **79**, 3637 (1997).

[20] E. Larose, L. Margerin, B. A. van Tiggelen, and M. Campillo, Phys. Rev. Lett. **93**, 048501 (2004).

[21] B. A. van Tiggelen, A. Lagendijk, and D. S. Wiersma, Phys. Rev. Lett. **84**, 4333 (2000).

[22] E. Abrahams, P. W. Anderson, D. C. Licciardello, and T. V. Ramakrishnan. Phys. Rev. Lett. **42**, 673 (1979).

[23] N. Cherroret, T. Karpiuk, C. A. Müller, B. Grémaud, and C. Miniatura, Phys. Rev. A **85**, 011604 (2012).

[24] S. Ghosh, N. Cherroret, B. Grémaud, C. Miniatura, D. Delande, Phys. Rev. A **90**, 063602 (2014).

[25] S. E. Skipetrov, A. Minguzzi, B. A. van Tiggelen, and B. Shapiro, Phys. Rev. Lett. **100**, 165301 (2008).

[26] S. Roche and D. Mayou, Phys. Rev. Lett. **79**, 2518 (1997).

[27] H. Fehske, J. Schleede, G. Schubert, G. Wellein, V. S. Filinov and A. R. Bishop, Phys. Lett. A **373**, 2182 (2009).

[28] S. John, Phys. Today **44** , 32 (1991).

[29] T. Ohysuki and T. Kawarabayashi, J. Phys. Soc. Jpn **66**, 314 (1997).

[30] A. McKinnon and B. Kramer, Z. Phys. B **53**, 1 (1983).

[31] F. Wegner, Z. Phys. **B25**, 327 (1976).

[32] $L(t)$ is nothing but the size of a system for which the Heisenberg time is equal to t.

[33] G. Lemarié, B. Grémaud, and D. Delande, Europhys. Lett. **87**, 37007 (2009).